Inorg. Chem. **2002**, *41*, 4852–4858

From Linear Inorganic Chains to Helices: Chirality in the $M(pyz)(H_2O)_2MoO_2F_4$ (M = Zn, Cd) Compounds

Paul A. Maggard, Amy L. Kopf, Charlotte L. Stern, and Kenneth R. Poeppelmeier*

Department of Chemistry, 2145 Sheridan Road, Northwestern University, Evanston, Illinois 60208-3113

Kang Min Ok and P. Shiv Halasyamani

Department of Chemistry, 4800 Calhoun Boulevard, University of Houston, Houston, Texas 77204-5003

Received March 5, 2002

$Cd(C_4H_4N_2)(H_2O)_2MoO_2F_4$ ($C_4H_4N_2$ = pyrazine, pyz) was synthesized via hydro(solvato)thermal methods and characterized by single-crystal X-ray diffraction methods (*P3*$_2$*21*, no. 154, $Z = 3$, $a = 7.4328(7)$ Å, $c = 16.376(2)$ Å). Both of the known $M(pyz)(H_2O)_2MoO_2F_4$ (M = Zn, Cd) compounds are comprised of *trans*-$M(pyz)_2(OH_2)_2F_2$ and *cis*-MoO_2F_4 octahedra that share fluoride vertices to form helical chains along the 3-fold screw axes. Individual chains are bridged to six symmetry-equivalent helices through metal–pyrazine and $OH_2\cdots F$ and $OH_2\cdots O$ hydrogen bonds. Structural comparisons of similar oxyfluoride chains demonstrate that they can be varied from linear to helical through (1) the replacement of pyridine or pyrazine by H_2O molecules and (2) the substitution of cis-directing $MoO_2F_4^{2-}$ anions in place of trans-directing $WO_2F_4^{2-}$ or TiF_6^{2-} anions. Infrared absorption (IR) measurements for M = Cd show two distinct O–H stretches corresponding to hydrogen-bonded O–H···F and O–H···O groups. Contrastingly for M = Zn, IR measurements exhibit O–H stretches for averaged hydrogen-bonded O–H···(O/F) groups, free (unbound) O–H groups, and higher energy Mo–F stretches. The IR data suggest a small fraction of the O–H···F hydrogen bonds are broken in the M = Zn analogue as a result of the racemic twinning. Both compounds exhibit nonlinear optical behavior, with second harmonic generation (SHG) intensities, relative to SiO_2, of ~0.25 ($\langle d_{ijk}^{2\omega}\rangle = 0.28$ pm/V) for the racemically twinned $Zn(pyz)(H_2O)_2MoO_2F_4$ and ~1.0 ($\langle d_{ijk}^{2\omega}\rangle = 0.55$ pm/V) for the enantiopure $Cd(pyz)(H_2O)_2MoO_2F_4$.

Introduction

To synthesize materials with desired physical or chemical properties, chemical reactions are often planned on controlling the topology of inorganic frameworks. Solids which have particular crystal classes, or molecules which have certain point groups, are required for many properties, such as reported for chirality, polarity, optical activity, and piezoelectricity/SHG,[1,2] the subcategories reflecting properties of noncentrosymmetric symmetries. The four categories of noncentrosymmetric properties overlap significantly, as highlighted in a recent review,[2] and a noncentrosymmetric compound may have one of seven possible combinations, such as grouping piezoelectricity and optical activity with chirality (as in 422), polarity (as in *mm*2), or both chirality and polarity (as in 2). To understand property relationships, such as when chirality and polarity occur together or separately, requires the rational synthesis of chemically similar but structurally different solid-state compounds.

Many interrelated and comparable metal−oxyfluoride compounds have been prepared with the use of similar anionic and cationic components, i.e., $(Ti/Zr)F_6^{2-}$, $(V/Nb/Ta)OF_5^{2-}$, or $(Mo/W)O_2F_4^{2-}$ and $(Cu/Zn/Cd)L_4^{2+}$ (L = pyridine, pyrazine, or other nitrogen-containing ligands), respectively. Compounds with similar compositions, but subtle structural changes, include the vertex-sharing chains in $Cu(py)_4MX_6$ ($MX_6 = TiF_6^{2-}$, ZrF_6^{2-}, HfF_6^{2-}, $NbOF_5^{2-}$,

* Author to whom correspondence should be addressed. E-mail: krp@northwestern.edu.

(1) *International Tables for Crystallography*; D. Reidel Publishing Company: Boston, MA, 1983; Vol. A, p 782.
(2) Halasyamani, P. Shiv.; Poeppelmeier, K. R. *Chem. Mater.* **1998**, *10*, 2753.

10.1021/ic0255712 CCC: $22.00 © 2002 American Chemical Society
Published on Web 07/24/2002

$TaOF_5^{2-}$, $WO_2F_4^{2-}$; py = pyridine),[3−5] $Cd(py)_4NbOF_5$,[6] $Cu(py)_2(H_2O)_2WO_2F_4$,[4] $Cu(py)_4TiF_6 \cdot 3H_2O$,[5] and $Cu(pyz)_2MX_6 \cdot (pyz)(H_2O)$ ($MX_6 = NbOF_5^{2-}$, $WO_2F_4^{2-}$),[7,8] as well as cluster geometries for $[pyH]_2[Cu(py)_4(MX_6)_2]$ ($MX_6 = TiF_6^{2-}$, ZrF_6^{2-}, HfF_6^{2-}, VOF_5^{2-}, $NbOF_5^{2-}$, $MoO_2F_4^{2-}$, $WO_2F_4^{2-}$),[5,9−10] $[pyH]_2[Cd(py)_4(NbOF_5)_2]$,[11] $[(HNC_6H_9OH)_2Cu(py)_4(WO_2F_4)_2]$,[12] and $(CuF(py)_4)_2NbOF_5$.[13] The structural features of these related compounds have been analyzed and the variables elucidated that regulate their solid-state structures, including the cis- or trans-directing nature of particular octahedral anions and cations,[5,10] and the coordination of pyridine,[3−6,9−11,13] pyrazine,[7,8] or 5-hydroxy-2-methylpyridine.[12]

The structure-directing features of these oxyflouride anions and ligand-coordinated cations have been utilized to meet two general conditions to synthesize a noncentrosymmetric solid-state structure: (1) the octahedra must crystallize without O/F disorder, which would result in metal-centered inversion sites, and (2) avoid inversion relations between neighboring oxyfluoride octahedra as well. The first condition can be met when protonated ligand cations $(pyH)^+$ and/or metal cations (Cu^{2+}, Zn^{2+}) coordinate to the oxide or fluoride sites on the early transition metal, so that as these larger cations pack in an ordered way, so too do the associated oxide and fluoride atoms.[9,12] For the second condition, we recently reported the combined effects of ligand length and helical symmetry on the extended assembly of the noncentrosymmetric and chiral phase, $Zn(pyz)(H_2O)_2MoO_2F_4$.[14] Reported herein, we further analyze the hydrogen bonding that occurs between the inorganic oxyfluoride chains and that influences the formation of racemic (inversion) twins for $Zn(pyz)(H_2O)_2MoO_2F_4$ but not for $Cd(pyz)(H_2O)_2MoO_2F_4$. The elimination of racemic twinning in a chiral compound corresponds to having an enantiopure crystal, and is an additional requirement to enhance the physical and chemical properties of a noncentrosymmetric material. Also reported here is the rational formation of helical oxyfluoride chains from linear chains, SHG intensities of both compounds, a racemic twinning model, and the roles of chirality and polarity in noncentrosymmetric chain structures.

Table 1. Selected Crystal and Refinement Data for $Cd(pyz)(H_2O)_2MoO_2F_4$

empirical formula	$Cd(C_4H_4N_2)(H_2O)_2MoO_2F_4$
fw	432.5
space group, Z	$P3_221$ (no. 154), 3
T, °C	153(2)
a, Å	7.4328(7)
b, Å	7.4328(7)
c, Å	16.376(2)
V, mm^3	783.5(2)
μ(Mo Kα), mm^{-1}	3.294
d_{calc}, g cm^{-3}	2.724
d_{exp},[a] g cm^{-3}	2.74(1)
Flack parameter	−0.01(6)
data/restraints/parameters	1265/0/76
final R1, wR2[b] [$I > 2\sigma(I)$]	0.0214, 0.0568

[a] Density measured by flotation pycnometry. [b] $R1 = \sum||F_o| - |F_c||/\sum|F_o|$; $wR2 = \{\sum[w(F_o^2 - F_c^2)^2]/\sum[w(F_o^2)^2]\}^{1/2}$, $w = \sigma_F^{-2}$.

Experimental Section

Caution. Hydrofluoric acid is toxic and corrosive!

Materials. CdO (99.99+%, Aldrich), MoO_3 (99.9995%, Alfa AESAR), pyrazine (99+%, Aldrich) and HF (aqueous, 49%, Aldrich) were used as received. Reagent amounts of deionized water were also used in the synthesis.

Synthesis. The synthesis of $Zn(pyz)(H_2O)_2MoO_2F_4$ has been reported previously.[14] $Cd(pyz)(H_2O)_2MoO_2F_4$ was similarly synthesized by adding 2.16×10^{-1} g (1.69×10^{-3} mol) of CdO, 2.43×10^{-1} g (1.69×10^{-3} mol) of MoO_3, 2.70×10^{-1} g (3.37×10^{-3} mol) of pyrazine, 1.20 g (3.37×10^{-2} mol) of 49% HF, and 7.59×10^{-2} g (4.21×10^{-3} mol) of H_2O to an FEP Teflon pouch. These pouches were heat sealed and placed inside a 125 mL autoclave (Parr) that was backfilled with ~42 mL of H_2O before closing. The autoclave was heated inside a furnace to 125 °C for 24 h and slowly cooled to room temperature at 6 °C/h. Transparent crystals of $Cd(pyz)(H_2O)_2MoO_2F_4$ were recovered by filtration in ~75% yield based on Cd.

Crystallographic Determination. Several cube-shaped crystals were examined under an optical microscope equipped with cross polarizers, and the best were selected for data collection on a Bruker CCD diffractometer operating at 153 K. The unit cell obtained was trigonal with $a = 7.4328(7)$ Å and $c = 16.376(2)$ Å. One sphere of reflections ($\pm h$, $\pm k$, $\pm l$) was collected and then processed with SAINTPLUS[15] to $2\theta = 56°$ to give 7149 reflections, of which 1265 were unique and $I > 2\sigma_I$. The structure was solved and refined with SHELXTL[16] in the trigonal space group $P3_221$ (no. 154) and checked for additional symmetry elements with the program PLATON.[17] Hydrogen atoms for each of the four carbon atoms on pyrazine were placed in idealized positions around the ring at a distance of 0.95 Å. Final anisotropic structure refinement converged at R1/*w*R2 = 0.021/0.057, with a data:variable ratio of ~17:1. The Flack parameter[18,19] converged at −0.01(6), which indicated the correct absolute structure and absence of racemic twinning. The hydrogen positions of the H_2O molecules were located in the final Fourier map and left unrefined. Some data collection and refinement parameters, as well as selected atomic coordinates and isotropic-equivalent displacement parameters, are given in Tables 1 and 2. Additional data collection, refinement and anisotropic displacement

(3) Halasyamani, P. Shiv.; Willis, M. J.; Stern, C. L.; Lundquist, P. M.; Wong, G. K.; Poeppelmeier, K. R. *Inorg. Chem.* **1996**, *35*, 1367.
(4) Halasyamani, P. Shiv.; Heier, K. R.; Stern, C. L.; Poeppelmeier, K. R. *Acta Crystallogr.* **1997**, *C53*, 1240.
(5) Norquist, A. J.; Heier, K. R.; Stern, C. L.; Poeppelmeier, K. R. *Inorg. Chem.* **1998**, *37*, 6495.
(6) Halasyamani, P. Shiv.; Heier, K. R.; Norquist, A. J.; Stern, C. L.; Poeppelmeier, K. R. *Inorg. Chem.* **1998**, *37*, 369.
(7) Halasyamani, P. Shiv.; Heier, K. R.; Willis, M. J.; Stern, C. L.; Poeppelmeier, K. R. *Z. Anorg. Allg. Chem.* **1996**, *622*, 479.
(8) Heier, K. R.; Norquist, A. J.; Halasyamani, P. Shiv.; Duarte, A.; Stern, C. L.; Poeppelmeier, K. R. *Inorg. Chem.* **1999**, *38*, 762.
(9) Heier, K. R.; Norquist, A. J.; Wilson, C. G.; Stern, C. L.; Poeppelmeier, K. R. *Inorg. Chem.* **1998**, *37*, 76.
(10) Welk, M. E.; Norquist, A. J.; Stern, C. L.; Poeppelmeier, K. R. *Inorg. Chem.* **2000**, *39*, 3946.
(11) Halasyamani, P. Shiv.; Willis, M. J.; Heier, K. R.; Stern, C. L.; Poeppelmeier, K. R. *Acta Crystallogr.* **1996**, *C52*, 2491.
(12) Welk, M. E.; Norquist, A. J.; Stern, C. L.; Poeppelmeier, K. R. *Inorg. Chem.* **2001**, *40*, 5479.
(13) Norquist, A. J.; Welk, M. E.; Stern, C. L.; Poeppelmeier, K. R. *Chem. Mater.* **2000**, *12*, 1905.
(14) Maggard, P. A.; Stern, C. L.; Poeppelmeier, K. R. *J. Am. Chem. Soc.* **2001**, *123*, 7742.
(15) *SAINTPLUS*; Bruker AXS, Inc.: Madison, WI, 1996.
(16) *SHELXTL*; Bruker, AXS, Inc.: Madison, WI, 1997.
(17) Spek, A. L. *PLATON*; Utrecht University: Utrecht, The Netherlands, 2001.
(18) Flack, H. D.; Bernardinelli, G. *J. Appl. Crystallogr.* **2000**, *33*, 1143.
(19) Flack, H. D.; Bernardinelli, G. *Acta Crystallogr.* **1999**, *A55*, 908.

Table 2. Selected Atomic Coordinates and Equivalent Isotropic Displacement Parameters ($Å^2 \times 10^3$) for $Cd(pyz)(H_2O)_2MoO_2F_4$

atom	Wyckoff symm.	*x*	*y*	*z*	*U*(eq)[a]
Mo	3a	0.46803(7)	0.46803(7)	0	18.1(1)
Cd	3b	0	0.25174(5)	5/6	13.6(1)
F1	6c	0.5209(6)	0.3504(6)	0.9030(2)	36.6(8)
F2[b]	6c	0.1720(4)	0.3403(5)	0.9538(1)	17.9(4)
O1	6c	0.5293(7)	0.7057(6)	0.9518(3)	44(1)
O2[b]	6c	0.6972(5)	0.1175(5)	0.9040(2)	24.0(7)
N1	3b	0	0.5647(6)	5/6	14(1)
N2	3b	0	0.9390(7)	5/6	15(1)
C1	6c	0.0771(8)	0.8843(7)	0.8964(3)	21.4(9)
C2	6c	0.0777(8)	0.6978(7)	0.8958(2)	20.7(9)

[a] *U*(eq) is defined as one-third of the trace of the orthogonalized U_{ij} tensor. [b] Coordinated to both Mo and Cd.

parameters, and all near-neighbor interatomic distances are given in the Supporting Information.

Spectroscopic Measurements. Mid-infrared (400−4000 cm^{-1}) spectra were collected on $M(pyz)(H_2O)_2MoO_2F_4$ (M = Zn, Cd) with a Bio-Rad FTS-60 FTIR spectrometer operating at a resolution of 2 cm^{-1}. Both samples were ground and pelletized with dried KBr, transferred to the FTIR spectrometer, and evacuated for 2 to 5 min before spectra acquisition.

Magnetic Susceptibility. Magnetization of polycrystalline samples of $M(pyz)(H_2O)_2MoO_2F_4$ (M = Zn, Cd), encased in sealed gelatin capsules, were measured from 5 to 300 K at a field of 1 kG with a Quantum Design Corp. MPMS SQUID susceptometer. The data were corrected for diamagnetism of both the sample holder and atomic cores.

Nonlinear Optical Measurements. Powder SHG measurements were performed on a modified Kurtz-NLO system with 1064 nm light.[20] A Continuum Minilite II laser, operating at 15 Hz (3 mJ average energy), was used for all measurements. No index matching fluid was used in the experiments. The SHG, i.e., 532 nm green light, radiation was collected in reflection and detected by a photomultiplier tube (Oriel Instruments). To detect only the SHG light, a 532 nm narrow band-pass interference filter was attached to the tube. A digital oscilloscope (Tektronix TDS 3032) was used to view the SHG signal.

Results and Discussion

Structural Description. The crystal structure of the racemically twinned $Zn(pyz)(H_2O)_2MoO_2F_4$, isostructural to the nontwinned $Cd(pyz)(H_2O)_2MoO_2F_4$ version here, has been described previously.[14] Selected interatomic distances and angles for both phases are listed together in Table 3, and those for $Cd(pyz)(H_2O)_2MoO_2F_4$ are also drawn in Figure 1. Both compounds share the same general structural features. A 3-fold screw axis passes down the middle of a helical chain comprising *cis*-MoO_2F_4 and *trans*-$M(pyz)_2(H_2O)_2F_2$ distorted octahedra that share fluoride vertices, Figure 1a. Perpendicular to the helical chains are 2-fold rotations that bisect each O−Mo−O angle.

Distances around the local Mo environment, identified before as an $MoO_2F_4^{2-}$ anion,[9,21] are similar in both phases. The *cis*-oxide distances to Mo are 1.774(4) (×2) and 1.749(3) Å (×2) for M = Cd and Zn, respectively, while the four Mo−F distances are 1.946(3) and 2.056(2) Å (×2 for each) for M = Cd and 1.932(2) and 2.060(2) Å (×2 for each) for M = Zn. In both compounds, Mo is displaced from the octahedron center toward the *cis*-oxide atoms, as seen for previously characterized $MoO_2F_4^{2-}$ anions.[9,14,21] The longer two of the four Mo−F distances are *trans* to the *cis*-oxides, and therefore, these two more nucleophilic fluorides are preferentially coordinated by either Cd or Zn cations to eliminate the potential O/F ligand disorder.[14] The coordination environment of the late transition metal is completed by two pyrazine molecules at 2.324(5) and 2.326(5) Å for

Table 3. Selected Interatomic Distances (Å) and Angles (deg) in $M(pyz)(H_2O)_2MoO_2F_4$ for M = Zn and Cd

			distance	
atom 1	atom 2	mult.	Cd	Zn
Mo	O1	2×	1.774(4)	1.749(3)
	F1	2×	1.946(3)	1.932(2)
	F2	2×	2.056(2)	2.060(2)
M	O2	2×	2.271(3)	2.049(2)
	F2	2×	2.262(2)	2.056(2)
	N1		2.324(5)	2.206(4)
	N2		2.326(5)	2.213(3)
H[a]	F1		1.81	1.85
(H-bonding)	O1		2.02	1.86

	degrees	
angle	Cd	Zn
F2−Mo−F2	80.0(2)	78.8(1)
Mo−F2−M	140.7(1)	142.28(9)
F2−M−F2	179.0(2)	179.7(1)

[a] Hydrogen atoms on H_2O were located in the final Fourier map and not refined.

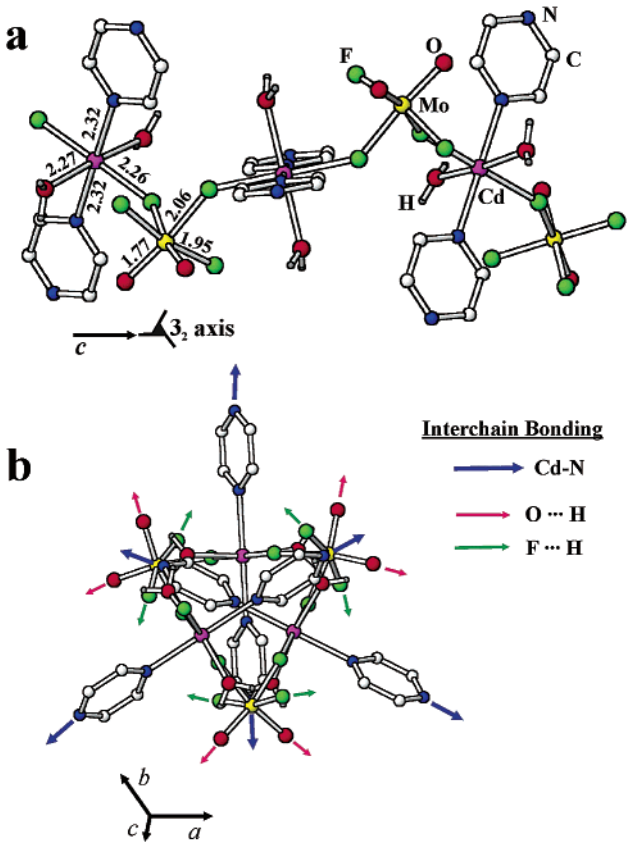

Figure 1. The helical chain repeat unit in $Cd(pyz)(H_2O)_2MoO_2F_4$ (a) viewed along the *c* axis with selected atoms and distances (in Å) labeled and (b) viewed down the *c* axis with interchain Cd−N, O···H, and F···H bonding labeled.

(20) Kurtz, S. K.; Perry, T. T. *J. Appl. Phys.* **1968**, *39*, 3798.
(21) Grandjean, D.; Weiss, R. *Bull. Soc. Chim. Fr.* **1967**, *8*, 3040.

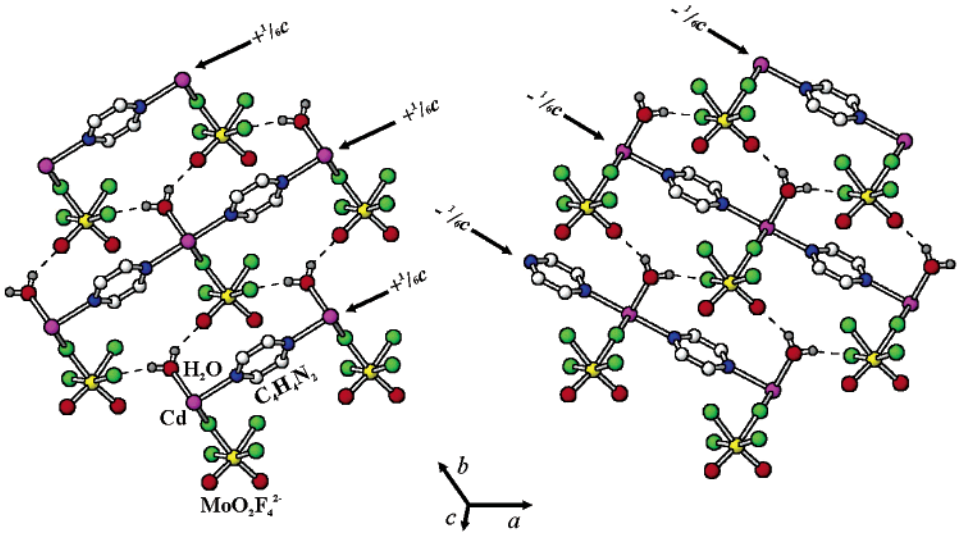

Figure 2. The packing of one layer of $MoO_2F_4^{2-}$ polyhedra with $Cd(pyz)(H_2O)_2^{2+}$ rows both above at $+1/6c$ (left) and below at $-1/6c$. Dashed lines indicate the O···H and F···H hydrogen bonds.

M = Cd, and 2.206(4) and 2.213(3) Å for M = Zn and two water molecules at 2.271(3) and 2.049(2) Å, respectively, as before, to give $M(pyz)_2(H_2O)_2F_2$ octahedra. The larger ionic size of Cd compared to Zn accounts for the relatively greater M−N, M−O, and M−F distances.

A view down the length of the chain, Figure 1b, illustrates the location of hydrogen bonding and covalent Zn/Cd−pyrazine bridges between a single helix and six neighbors. Each helical chain has covalent M−pyrazine bridges spaced every 60° (blue arrows), or six per helix rotation, with three extending from the perimeter of the helix and three extending through the middle of the helix, in an alternating arrangement. Metal−pyrazine bridges that extend through the helix center allow for H_2O molecules, which are coordinated on neighboring chains, to hydrogen bond to oxide or fluoride atoms on the MoO_2F_4 octahedra (red and green arrows). Shown in Figure 2, the $M(pyz)_2(OH_2)_2F_2$ octahedra are aligned with the M−pyrazine bonds parallel to the *ab* plane, while the M−OH_2···(F/O) hydrogen bonds are directed at the MoO_2F_4 octahedra from both above ($+1/6c$, left) and below ($-1/6c$, right). Each helical chain forms six F···H−O and six O···H−O hydrogen bonds per helix rotation, Figure 1b, at 1.81 and 2.02 Å (×3 for each) for M = Cd and 1.85 and 1.86 Å (×3 for each) for M = Zn, respectively, and also donates to neighboring chains a symmetry-equivalent number of O−H···F/O hydrogen bonds, spaced 120° apart. The O−H···(F/O) hydrogen bonds are relatively more asymmetric for the M = Cd analogue, with an ~0.2 Å longer O−H···O distance versus O−H···F. This difference is a result of the longer Cd−pyrazine bond distances, relative to Zn−pyrazine, that space the helices apart further (as reflected in the increased *a* (=*b*) unit cell dimension).

Infrared Measurements. The observed infrared bands are in good agreement with those reported for analogous compounds containing *cis*-MoO_2F_4,[22,23] pyrazine,[24,25] and free

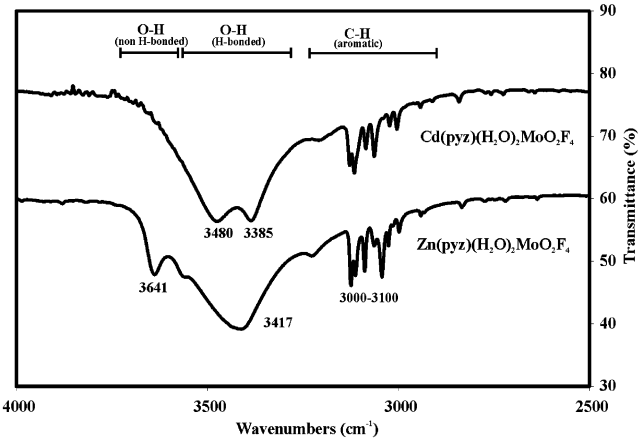

Figure 3. The infrared transmittance spectra for the $M(pyz)(H_2O)_2MoO_2F_4$ (M = Zn, Cd) phases between 2500 and 4000 cm^{-1}, which are labeled to show the O−H (both free and hydrogen bonded) and C−H (aromatic) stretching regions

or hydrogen-bonded H_2O.[24,25] The Mo−O symmetric and antisymmetric stretching frequencies were identified at 952 and 909 cm^{-1} for M = Zn and 954 and 913 cm^{-1} for M = Cd, while the Mo−F stretching frequencies for each are observed as slightly broader peaks at 568 and 547 cm^{-1}, respectively, as before. The Mo−O stretches for the M = Zn and Cd analogues match closely in energy, ±2−4 cm^{-1}, while the Mo−F stretches for the M = Zn analogue are displaced to a higher energy by 21 cm^{-1}. The latter difference is owing to broken O−H···F hydrogen bonds and therefore strengthened Mo−F bonds (below).

Hydrogen bonding between neighboring helical chains in the M = Zn and Cd compounds has additional subtle differences, as shown in the transmittance spectra in Figure 3. The M = Cd analogue exhibits two O−H stretches in the region for hydrogen-bonded groups, at 3480 and 3385 cm^{-1}, consistent with the shorter fluoride and longer oxide hydro-

(22) Kharitonov, Yu. Ya.; Buslaev, Yu. A.; Kuznetsova, A. A. *Zh. Neorgan. Khim.* **1966**, *11*, 821.
(23) Pausewang, G.; Schmitt, R.; Dehicke, K. *Z. Anorg. Allg. Chem.* **1974**, *408*, 1.
(24) Nakamoto, K. *Infrared and Raman Spectra of Inorganic and Coordination Compounds, Part A*; John Wiley & Sons: New York, 1997.
(25) Pouchert C. J. *The Aldrich Library of FT-IR Spectra*; Aldrich Chemical Co.: Milwaukee, WI, 1997.

gen bonds, Table 3. However, in the M = Zn analogue, the hydrogen bond distances to the fluoride and oxide atoms are nearly equivalent, leading to an averaged hydrogen-bonded O−H stretch at 3417 cm^{-1}. An extra O−H stretch at 3641 cm^{-1} is also present in the energy range expected for non-hydrogen-bonded O−H groups, and is a result of broken O−H···F hydrogen bonds in the racemically twinned M = Zn phase, the mechanism for which is described below. In the nontwinned M = Cd version there are stronger and shorter O−H···F hydrogen bonds, and the racemic twinning is eliminated.

Magnetic and Nonlinear Optical Properties. After diamagnetic corrections, both $M(pyz)(H_2O)_2MoO_2F_4$ compounds have a small temperature-independent paramagnetic susceptibility of 8.48×10^{-5} emu/mol for M = Zn and 7.47×10^{-5} emu/mol for M = Cd, with a very small temperature dependence at <50 K. Before correction for the atomic cores both samples are appropriately diamagnetic, consistent with that expected for Cd^{2+}/Zn^{2+} and Mo^{6+} (d^0) ions.

The $M(pyz)(H_2O)_2MoO_2F_4$ compounds exhibit SHG intensities approximately 0.25 and 1.0 to that in α-quartz for M = Zn and Cd, respectively. The average NLO susceptibilities correspond to 0.28 and 0.55 pm/V ($\langle d_{ijk}^{2\omega} \rangle$), respectively, which are calculated from the Kurtz powder (SHG) measurements, as reported.[26] The weaker SHG response of the M = Zn analogue is a result of the racemic twinning, compared to its absence in the enantiopure M = Cd version. Also, the relatively low SHG intensity of both phases, compared to that known for the commercially used $LiNbO_3$ solid,[27] is correlated with the absence of a net dipole moment in the structure. To generate a stronger SHG response, the individual atomic polarizations (β) should constructively add,[26,28] but the dipole moments of the $MoO_2F_4^{2-}$ octahedra are self-canceling within each helical chain (described below). Phase matching cuves, or SHG versus particle size, were performed for both phases and plotted in Figure 4. The M = Zn and Cd solids are both non-phase-matchable, with SHG intensities peaking at a particle size of approximately 45−63 μm. Additional single-crystal SHG measurements could be insightful, especially in regards to the racemic twinning model (below), in the future.

Racemic Twinning Model. Although both $Zn(pyz)(H_2O)_2MoO_2F_4$ and $Cd(pyz)(H_2O)_2MoO_2F_4$ have similar structures and compositions, crystals for the M = Zn analogue are racemically twinned at an ~50% ratio and have an SHG intensity about 4 times smaller than the M = Cd analogue. A model of the twin boundary is necessary to understand the structural features that determine whether twin formation occurs, i.e., enantiopurity, as well as to understand the broken O−H···F hydrogen bonds for M = Zn, which is reflected in the displaced O−H and Mo−F stretching energies relative to the M = Cd phase.

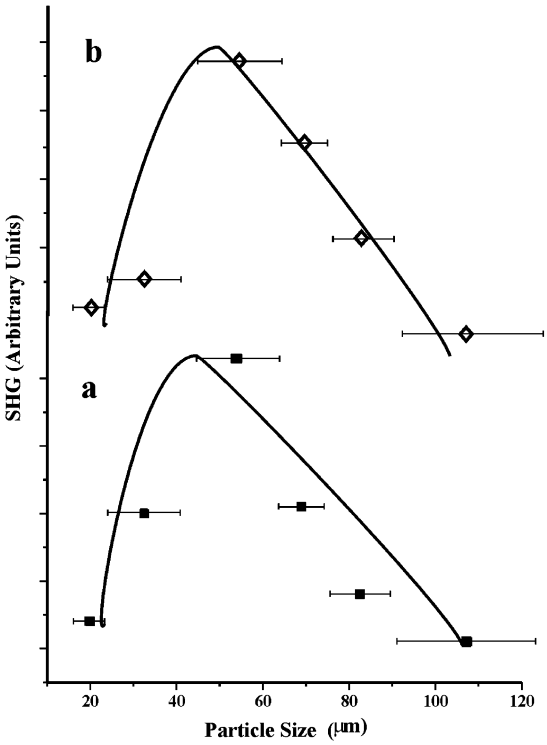

Figure 4. Phase matching curves, particle size vs SHG intensity, for (a) $Zn(pyz)(H_2O)_2MoO_2F_4$ and (b) $Cd(pyz)(H_2O)_2MoO_2F_4$. The drawn curves are to guide the eye and are not a fit to the data.

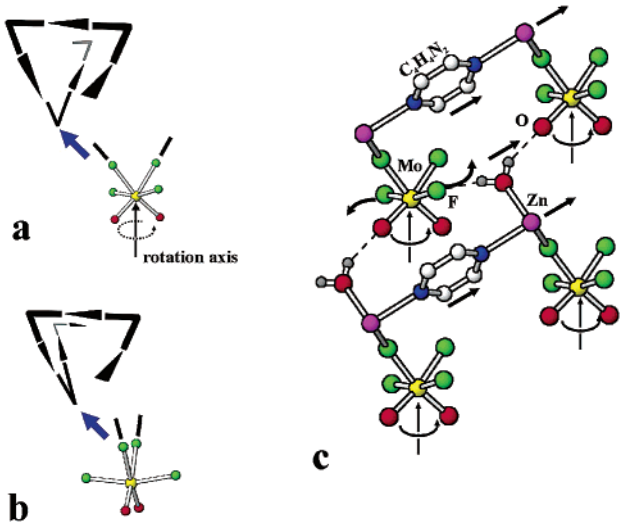

Figure 5. Twinning mechanism for the conversion of a left-handed helix (a) to a helix with both left- and right-handed sections (b) by rotating a MoO_2F_4 vertex counter-clockwise around the O−Mo−O angle. The correlated movements of the Zn, pyrazine, H_2O, oxide, and fluoride groups are shown in (c) with arrows.

As the racemic, or inversion, twin of a left-handed helix in $Zn(pyz)(H_2O)_2MoO_2F_4$ is a right-handed helix, the twinning mechanism should account for both types of helices in the same crystal. Described in the earlier communication on $Zn(pyz)(H_2O)_2MoO_2F_4$,[14] the packing of opposite-handed helical chains parallel to each other would result in uncoordinated Zn^{2+} and broken O−H···F/O hydrogen bonds between and down the entire length of the inorganic helices. A more probable twinning model is drawn in Figure 5, which leaves the O−H···O hydrogen bonds and covalent Zn−

(26) Porter, Y.; Ok, K. M.; Bhuvanesh, N. S. P.; Halasyamani, P. S. *Chem. Mater.* **2001**, *13*, 1910.
(27) Smolenskii, G. A.; Kozhevnikova, N. V. *Dokl. Akad. Nauk S.S.S.R.* **1951**, *76*, 519.
(28) Jeggo, C. R.; Boyd, G. D. *J. Appl. Phys.* **1970**, *41*, 2741.

pyrazine bonds intact, and therefore is consistent with the IR data. The proposed model to convert a left-handed helix, Figure 5a, to a helix with both left- and right-handed sections, Figure 5b, is to rotate one MoO_2F_4 vertex in the helix counterclockwise about an axis bisecting the O−Mo−O angle. The imagined rotation of the MoO_2F_4 vertex is a visualization of the twin boundary that occurs when crystals of opposite handed helices grow together, not a proposed internal distortion. The twin boundary in $Zn(pyz)(H_2O)_2MoO_2F_4$, which is comprised of bundles of interleaved helices, is therefore imagined as a single layer of rotated vertices that connects right- and left-handed sections down the length of the chains.

A layer of MoO_2F_4 vertices, each the vertex of separate helical chain, is drawn in Figure 5c with arrows to help visualize the structural changes at the twin boundary. The drawn Zn−pyrazine layer is located above the plane of the page at $+1/6c$, the MoO_2F_4 octahedra are located below the plane of the page, and the O/F···H hydrogen bonds are directed between the two layers. As the MoO_2F_4 vertices are rotated counterclockwise around the O−Mo−O angle, to the final orientation of the twin boundary as in Figure 5b, the coordinated Zn atoms are displaced in the same direction, i.e., those at $+1/6c$ in Figure 5c move to the right and up. Also coordinated to Zn, the H_2O and pyrazine molecules are displaced in the same direction by the anion rotation. The H···F hydrogen bonds are broken as the H_2O molecules are displaced away from the associated fluoride atoms, which rotate into the page. Contrastingly, the hydrogen-bonded oxide···H−O pairs are displaced in the same direction and are not broken at the twin boundary.

The above twinning model is consistent with the experimental infrared absorption data. The free O−H groups, resulting from the broken O−H···F hydrogen bonds, are observed as a small peak in the racemically twinned $Zn(pyz)(H_2O)_2MoO_2F_4$ compound, but not for $Cd(pyz)(H_2O)_2MoO_2F_4$. Furthermore, the Mo−F stretching frequencies are shifted to higher energies for the Zn analogue, as a result that when the O−H···F hydrogen bonds are broken, the Mo−F bonds are strengthened. Stronger and shorter O−H···F hydrogen bonds are present in the M = Cd analogue, and therefore racemic twinning does not occur. The Mo−O stretching frequencies are similar for the M = Cd and Zn compounds ($\pm 2-4$ cm^{-1}, compared to ± 21 cm^{-1} for Mo−F), consistent with our model.

Chirality and Polarity. Chirality has been the most obvious structural feature of interest in the $M(pyz)(H_2O)_2MoO_2F_4$ (M = Zn, Cd) compounds, as the chain packing suggested a direct route from chiral helical chains to chiral 3D packing.[14] Not so obvious, though, are the prominent structural features which lead to the formation of helical chains. Shown in Figure 6, the progression from linear to helical metal−oxyfluoride chains can be attributed to a particular combination of atomic and ligand substitutions. The $Cu(py)_4MX_6$[3−5] compounds have Cu and M ions that are both trans-directing and have no interchain hydrogen or metal−ligand bonding, and form the linear centric chain in Figure 6a. The substitution of two H_2O molecules for two

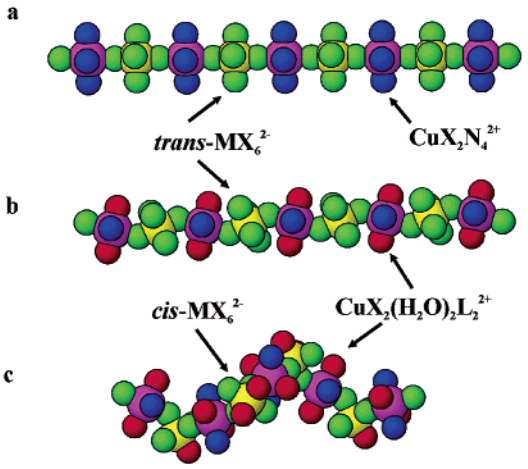

Figure 6. The progression of a linear chain as in (a) $Cu(py)_4MX_6$ (MX_6 = TiF_6^{2-}, ZrF_6^{2-}, HfF_6^{2-}, $NbOF_5^{2-}$, $TaOF_5^{2-}$, $WO_2F_4^{2-}$; py = pyridine)[3−5] to a zigzag chain in (b) $Cu(py)_2(H_2O)_2WO_2F_4$,[4] and $Cu(pyz)(H_2O)_2TiF_6$[29] to a helical chain in (c) $M(pyz)(H_2O)_2MoO_2F_4$ (M = Zn, Cd).

pyrazine or pyridine on the late transition metal site in $Cu(py)_2(H_2O)_2WO_2F_4$ or $Cu(pyz)(H_2O)_2TiF_6$[4,29] produces a bent W−F−Cu or Ti−F−Cu (140° for both) coordination, as the addition of inter- and intrachain hydrogen bonding now leads to the zigzag chain in Figure 6b. The metal−oxyfluoride zigzag chain lacks a rotational component that is required by any inorganic or organic helix.[30] In Figure 6c, the cis-coordinated $MoO_2F_4^{2-}$ anions, in place of the trans-coordinated $WO_2F_4^{2-}$ or TiF_6^{2-} anions in Figure 6b, lead to metal−oxyfluoride helices in $M(pyz)(H_2O)_2MoO_2F_4$. Shown more clearly in Figure 1b, the cis-coordinated $MoO_2F_4^{2-}$ anion primarily "turns" the chain (~60°), while the bent (141−142°) Mo−F−Zn/Cd coordination translates the chain.

Recent papers have started to highlight the importance of understanding the structure−property relationship between chirality and polarity,[2,31] such as to determine how a chiral molecule or chain might influence the net dipole moment of a structure. The chiral helical chains in $M(pyz)(H_2O)_2MoO_2F_4$ (M = Zn, Cd) are not polar as a result that the orientation of the dipole moments in the $MoO_2F_4^{2-}$ anions are perpendicular to the screw axis, which rotates the dipole vector at 120° intervals and averages the net dipole moment to zero. The rotational symmetry of a screw axis will effectively average to zero any dipole moment that is perpendicular to the rotation axis, and is analogous to the rule that a net dipole moment in a structure must remain unchanged by every symmetry element of the space group.[32] Therefore, the dipole moment of the anion must have a component that is collinear with the screw axis of the helical chain to give a net polar structure, such as known (below) for chains with trans-directing anions such as $NbOF_5^{2-}$ or $TaOF_5^{2-}$.

The recently reported $Cu(dpa)_2MOF_5 \cdot 2H_2O$ (dpa = 2,2′-dipyridylamine; M = Nb, Ta)[33] compound has helical chains

(29) Maggard, P. A.; Kopf, A. L.; Stern, C. L.; Poeppelmeier, K. R. Unpublished research.
(30) Lauer, J. L. *J. Chem. Phys.* **1959**, *30*, 1165.
(31) Paci, I.; Cann, N. M. *J. Chem. Phys.* **2001**, *115*, 8489.
(32) Drago, R. S. *Physical Methods for Chemists*; Saunders College Publishing: New York, 1992.

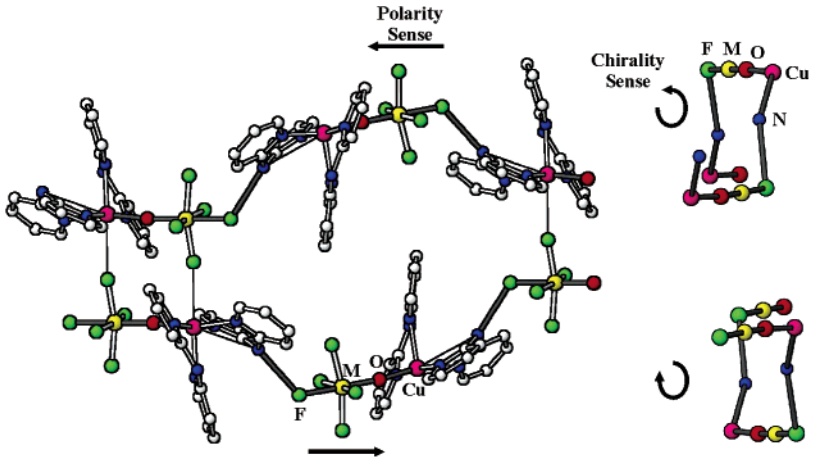

Figure 7. The polar and chiral metal−oxyfluoride chains in $Cu(2,2'\text{-dpa})_2MOF_5 \cdot 2H_2O$ (M = Nb, Ta; dpa = dipyridylammine).[33] The backbone of the helical chain F−M−O−Cu−N is drawn on the right, excluding the organic ligand.

that are individually both chiral and polar, shown in Figure 7. Compared to the $M(pyz)(H_2O)_2MoO_2F_4$ phases, the cis-directing anion, $MoO_2F_4^{2-}$, is replaced by the trans-directing $NbOF_5^{2-}$ and $TaOF_5^{2-}$ anions. The right side of Figure 7 shows the F−(Nb or Ta)−O−Cu−N backbone of the helical chain that propagates down a 2_1 screw axis. The F−N atoms are connected through a hydrogen bond (**F**···H−**N**) and the Cu−N atoms are connected through the dpa ligand (**Cu**−N_2C_{10}**N**H). The helical $Cu(dpa)_2MOF_5$ chains are not efficiently packed, and comprise a left-handed helix of one polarity sense and a right-handed helix of the opposite polarity sense to give a centrosymmetric (neither polar or chiral) structure. In analogy to the packing of the helical $M(pyz)(H_2O)_2MoO_2F_4$ chains,[14] if the $Cu(dpa)_2MOF_5$ helices were restricted to a single chirality sense, i.e., all left- or right-handed, a structure both polar and chiral would result. Alternatively, if every other $Cu(dpa)_2MOF_5$ helix were rotated by 180°, i.e., to the opposite polarity sense, a chiral structure would result, as the dipole moments of same-handed chains would average to zero. Solid-state compounds with both a polarity sense and a coincident chirality sense include $LiIO_3$[34] in space group $P6_3$ and Te_2O_5 in $P2_1$,[35] and have strong SHG intensities of 300 and 400 × SiO_2. Ongoing investigations are focused on synthesizing materials with an efficient SHG response through having both a chiral and a polar structure.

(33) Norquist, A. J.; Stern, C. L.; Poeppelmeier, K. R. *Inorg. Chem.* **1999**, *38*, 3448.
(34) Rosenzweig, A.; Morosin, B. *Acta Crystallogr.* **1966**, *20*, 758.
(35) (a) Lindqvist, O.; Moret, J. *Acta Crystallogr.* **1973**, *B29*, 643. (b) Porter, Y.; Ok, K. M.; Bhuvanesh, N. S. P.; Halasyamani, P. Shiv. *Chem. Mater.* **2001**, *13*, 1910.

Conclusions

$Cd(pyz)(H_2O)_2MoO_2F_4$ was synthesized via hydro(solvato)thermal methods and characterized by single-crystal diffraction to have helical chains comprising alternating *trans*-$Cd(pyz)_2(OH_2)_2(F)_2$ and *cis*-MoO_2F_4 octahedra that link through shared fluoride vertices. Structural comparisons between similar oxyfluoride chains demonstrate that they can be varied from linear to helical through (1) the replacement of pyridine or pyrazine by H_2O molecules and (2) the substitution of cis-directing $MoO_2F_4^{2-}$ anions in place of trans-directing $WO_2F_4^{2-}$ or TiF_6^{2-} anions. Analysis of the hydrogen bonding and Mo−(O/F) stretching frequencies leads to a twinning mechanism likely responsible for the racemic twinning in the $Zn(pyz)(H_2O)_2MoO_2F_4$ analogue, a reversal of the helical handedness at the twin boundary that leaves broken O−H···F hydrogen bonds.

Acknowledgment. The authors gratefully acknowledge support from the National Science Foundation (NSF), Solid State Chemistry (Award No. DMR-9727516), and made use of the Central Facilities supported by the MRSEC program of the National Science Foundation (Grant DMR-0076097) at the Materials Research Center of Northwestern University. P.S.H. thanks the Robert A. Welch Foundation and the NSF-Career Program (DMR-0092054) for support.

Supporting Information Available: X-ray crystallographic files, in CIF format, including tables of crystallographic details, atomic coordinates, anisotropic thermal parameters, and interatomic distances and angles. This material is available free of charge via the Internet at http://pubs.acs.org.

IC0255712